



A review of investigations on ground support requirements in coal burst-prone mines

Chunchen Wei¹ · Chengguo Zhang¹ · Ismet Canbulat¹ · Zhengyang Song² · Lianpeng Dai³

Received: 26 October 2021 / Accepted: 11 February 2022
© The Author(s) 2022

Abstract

Ground support is widely implemented to mitigate dynamic rock failures in underground mines. This paper investigated the ground support requirements in burst-prone mines to mitigate the catastrophic dynamic rock failures of rock and/or coal bursts. First, the ground support principles and considerations in burst-prone conditions are identified. The objective of a ground support system is to increase the capacity to accommodate rock fracturing in a rockburst and, in turn, to minimize the kinetic energy of the ejected material. The support capacities of various yielding rockbolts and integrated support systems are then investigated using the test results in the laboratory. Apart from the energy absorption and yielding deformation capacity, the initial stiffness and energy absorption rate are also critical factors when applying yielding rockbolts in practice. Adding rope lacing and mesh strap to surface support elements can substantially enhance the support performance of the system. In practice, semi-analytical and empirical approaches are often used to determine the ground support elements in burst-prone areas. Semi-analytical methods first evaluate the support demand in burst risk zones and then select support elements according to their laboratory test results. Alternatively, empirical methods determine the ground support elements according to the locally established empirical rating scheme, which usually ranks the support capacities of various support systems based on ground support conditions and damage conditions. The outcomes of this study can provide insights into ground support strategies and assist the mining industry to develop effective coal burst control technologies.

Keywords Coal burst · Dynamic ground support · Support capacity · Best-practice support design

1 Introduction

Rockburst is a term used to characterize rock dynamic failure associated with a large amount of energy released in a sudden and violent manner. In a rockburst, the fragmented rock blocks are rapidly ejected into excavations. Rockburst has been regarded as a major challenge in especially deep underground excavations for decades (Ortlepp 2005; Kaiser

and Cai 2012; Jiang et al. 2014; Suorinen et al. 2014; Iannacchione and Tadolini 2016; Mark 2016; Zhang et al. 2017; Zhou et al. 2018; Si and Belle 2019; Si et al. 2020; Song et al. 2020, 2021; Wei et al. 2020, 2021; Cai et al. 2021; Dai et al. 2021), because it is extremely difficult to predict and control. A rockburst is commonly termed a coal burst in underground coal mining and specifically refers to coal as the type of ejected material. It is of note that coal burst is different from outburst. The term outburst refers to coal ejection mainly driven by gas pressure in the coal, whereas no or minimal gas pressure is involved in a coal burst event (Hebblewhite and Galvin 2017; Wei et al. 2018). In Australia, coal bursts are relatively rare; however, the occurrence of coal bursts appears to be increasing, particularly as mine excavations go deeper. The first officially reported coal burst in Australia in 2014 caused two fatalities in a longwall gate road under construction (Hebblewhite and Galvin 2017).

For outburst, gas drainage is one of the main control measures. For coal burst-prone mines, various destressing techniques are applied to mitigate burst risks

✉ Chengguo Zhang
chengguo.zhang@unsw.edu.au

¹ School of Minerals and Energy Resources Engineering, University of New South Wales, Sydney, NSW 2052, Australia

² Department of Civil Engineering, School of Civil and Resource Engineering, University of Science and Technology Beijing, Beijing 100083, China

³ Key Laboratory of Ministry of Education on Safe Mining of Deep Metal Mines, Northeastern University, Shenyang 110819, China

(Iannacchione and Zelanko 1995; Konicek et al. 2011; He et al. 2012a; Dou et al. 2017; Jiang et al. 2017; Wei et al. 2018; Zuo et al. 2019), mainly including borehole blasting, destressing boreholes, shotfiring, water infusion, and hydraulic fracturing. These destressing approaches aim to produce a relatively ‘weak’ zone to relieve the high stresses or to soften the system to reduce the strain energy stored around excavations. However, each of these destressing approaches has certain limitations in field implementation (Wei et al. 2018). In comparison, ground support is an alternative operational control that is more widely applied for burst-prone mines as it is applicable for broader geological and geotechnical underground conditions.

Ground support techniques consist of two main components: support and reinforcement (Thompson et al. 2012; Potvin and Hadjigeorgiou 2020). Support refers to the application of support load at the excavation surface through surface support elements, such as mesh and shotcrete. Reinforcement aims to strengthen the overall rock mass properties by installing support elements within the rock mass, such as installing rockbolts and cable bolts in boreholes. A ground support system refers to the application of both surface support elements and reinforcements to stabilize the excavations.

Numerous studies have investigated static and dynamic support capacities of various yielding rockbolts in laboratory tests (Li et al. 2014; Villaescusa et al. 2015; Masoudi and Sharifzadeh 2018; Smith et al. 2019; Sharifzadeh et al. 2020; Chen and Li 2021; Chen et al. 2021; Li et al. 2021). However, Cai (2013) pointed out that the support capacity of the integrated support system, instead of individual support elements, should be one of the main focuses in practice due to the existence of the ‘weakest link’ in the system. Thus, a number of scholars conducted drop tests and simulated rockburst experiments using blasting tests to focus on the support performance of integrated support systems (Ortlepp and Stacey 1998; Stacey and Ortlepp 2001; Hadjigeorgiou and Potvin 2007, 2011; Heal 2010; Bucher et al. 2013; Brändle et al. 2017). The support capacities of various ground support systems are also evaluated and rated in burst-prone mines to provide empirical guidance in ground support selection (Heal et al. 2006; Potvin 2009; Mikula 2012; Duan et al. 2015a; NGI 2015; Morissette and Hadjigeorgiou 2019).

This study investigates the ground support requirements in coal burst-prone mines, aiming to minimize the damage caused by catastrophic dynamic failures (i.e., coal burst and rockburst) and enhance the safety of the mining workforce. Section 2 evaluates and characterizes ground support principles and considerations in burst-prone conditions. Section 3 assesses support capacities (e.g., energy absorption, load capacities) of various yielding rockbolts and ground support systems. Section 4 reviews international best-practice

ground support systems in burst-prone coal and hard rock mines. The objectives of this study are to deepen the understanding of ground support strategies to assist the mining industry to develop effective coal burst control technologies.

2 Coal burst mechanisms and the associated demand on the ground support system

2.1 Coal burst and classification

Various terminologies and categorical methods have been used to classify rockbursts due to the complex rockburst mechanisms. Ortlepp and Stacey (1994) categorized rockbursts into five types: strain burst, buckling, face crush, shear rupture and fault-slip burst. In addition, they pointed out that rockburst mechanisms can be classified into source mechanisms and damage mechanisms, as the rockburst and the seismic event are not necessarily one and the same event (Ortlepp 1997, 2005). Hedley (1992) proposed a rockburst classification method for an underground hard rock mine, with three types of rockbursts: strain burst, pillar burst and fault-slip burst. Figure 1 shows schematic illustrations of the three types of rockbursts. This concise classification concept was generally accepted and was further developed by other researchers (Kaiser et al. 1992, 1996; Tang 2000; Castro et al. 2012; Gao et al. 2019; Vardar 2019). The buckling burst and shear rupture proposed by Ortlepp can then be grouped into strain burst and fault-slip burst, respectively (Kaiser and Cai 2012).

Strain burst usually occurs in the vicinity of highly stressed excavations, where the country rock is fracturing or spalling. The fracturing rock releases some amount of strain energy in the form of seismic waves that radiate out from the fracturing site. Strain burst occurs when a large

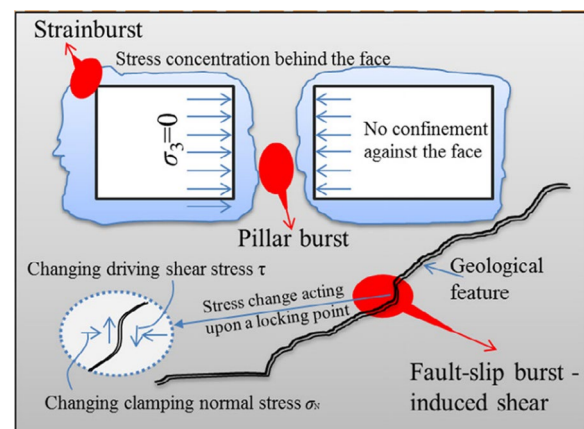


Fig. 1 Classification of rockbursts, after Castro et al (2012) and Zhou et al (2018)

amount of strain energy rapidly converts to kinetic energy and expels the rock or coal mass into the excavations resulting in damage and/or personnel injuries (Galvin 2016). The ejection velocity can reach as high as 100 m/s (Galvin 2016), although the energy magnitude of the corresponding seismic events is relatively low compared to other types of rockbursts (Ortlepp 1997, 2005). Pillar burst refers to a sudden collapse of the whole pillar involving a violent release of a large amount of strain energy within the pillar core section (Salamon and Wagner 1979; Cai and Kaiser 2018). Several studies classified pillar burst as strain burst since the mechanisms of the two burst types are associated with the sudden mining-induced unstable state of equilibrium, which releases a large amount of strain energy in a violent manner (Tang 2000; Simon 2001; He et al. 2012b; Galvin 2016), resulting in significant damage to rock support systems.

Both strain burst and pillar burst can be triggered by remote seismic events. The seismic waves (with seismic energy) produced by the remote seismic events can propagate to the highly stressed rock mass around excavations, resulting in rockbursts. In this scenario, the seismically triggered strain and pillar bursts are also named variously as combined rockbursts (Tang 2000), impact-induced bursts (He et al. 2012b) or triggered or induced rockbursts (Deng and Gu 2018). For the majority of seismically triggered strain and pillar bursts, the damage level is mainly determined by the amount of strain energy stored within the surrounding rock of excavations instead of the ‘trigger’ seismic energy (Ortlepp 1997; Galvin 2016). However, if the magnitude of seismic energy is considerably high, the rockbursts are more conventionally called fault-slip rockbursts, where the magnitude of seismic events can reach as high as 5.0 of Richter magnitude (Ortlepp and Stacey 1994). Therefore, fault-slip bursts refer to rockbursts caused by a sudden slippage along a geological fault, or, in a broad sense, along geological discontinuities. The discontinuities

mainly include joints and bedding planes within rock mass and weak contacts between geological discontinuities (e.g., fault and dyke) and the surrounding rock.

As shown in Fig. 2a, for a strain burst, the ejected rock is mostly characterized as thin plates with knife-sharp edges, as the strain burst is often self-initiated resulting from excessive tangential stress around excavations. The strain energy released from the intact rock is the main contributor to the ejected rock. In comparison, for a fault-slip burst (i.e., a strain burst triggered by a remote significant fault-slip), seismic stress waves trigger the strain burst, although the tangential stress is not greater than the rock strength around excavations. The seismic waves also contribute to the ejected rock resulting in heavily fragmented rock pieces with a wide range of sizes. The ejected rock debris ranges from finer rock blocks to large cubic blocks (as shown in Fig. 2b), which is different from the shape of ejected rock in a strain burst (Li 2021). Furthermore, it is observed that the boundary of the damaged zone is often associated with sudden condition changes, such as changes of lithology, presence of weak rock contacts, and significant changes in support layout (Li et al. 2019).

2.2 Ground support for burst-prone areas

Ground conditions can generally be divided into low-stress conditions and high-stress conditions (Li 2017a; Li et al. 2020; Potvin and Hadjigeorgiou 2020; Xue et al. 2020; Zhang et al. 2020). The instability of excavations at low-stress conditions is mainly related to the gravity of loosened rock blocks driven by the surrounding geological structures. The support system aims to provide enough support load to bear the deadweight. In comparison, the main task for a support system in high-stress conditions is to prevent rock failure around excavations caused by high-stress concentration (Kaiser and Cai 2012; Potvin and Hadjigeorgiou 2020).



(a) A self-initiated strain burst occurred in a hard quartzite mine with 1000 m of mining depth



(b) A strain burst triggered by a fault-slip seismicity event (i.e., fault-slip burst event) in a metal mine at 1100 m of mining depth

Fig. 2 Characteristics of damage zones of different types of rockbursts (Li 2021)

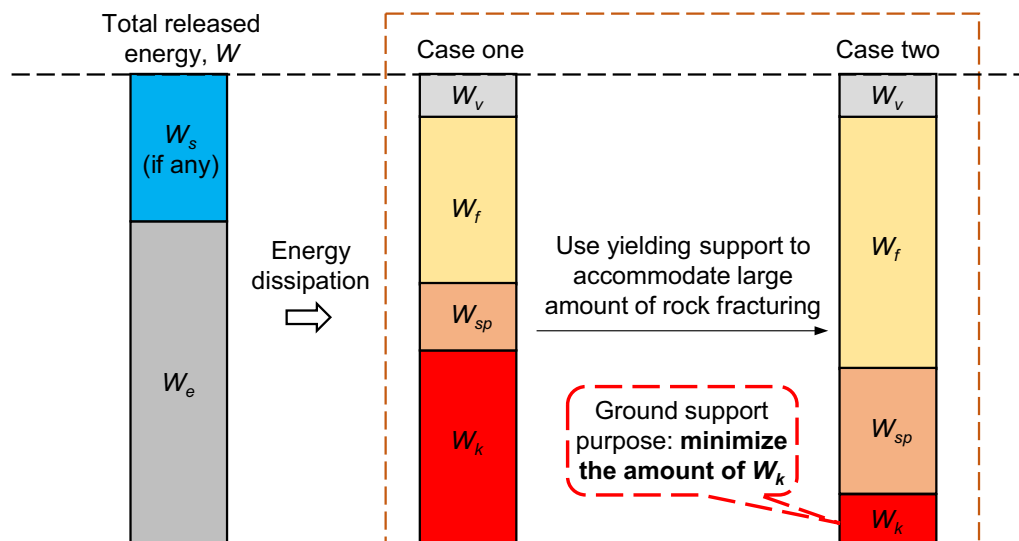


Fig. 3 Illustration of energy transformation in a rockburst, according to Li (2021). Note: the energy columns are not to scale

Furthermore, the rock mass failure can be sudden and violent, resulting in rockbursts. In this scenario, the ground support system is first required to have a stiff loading capacity to provide confinement to maintain the inherent strength of the rock mass to support itself. It is also crucial to provide considerable deformation capacity to hold the bulking (failed) or ejected rock mass and its deadweight (Cai 2013; Jiang et al. 2014).

The total released energy (W) in a rockburst consists of released strain energy (W_e) within country rock of excavations and, if any, the seismic energy (W_s) produced by remote seismic events (Li 2021), as shown in Fig. 3. For supported rock mass, the total released energy can be dissipated in four ways: rock fracturing (W_f), rock vibration and heat (W_v), rock support system (W_{sp}), and kinetic energy (W_k) of rock ejection (if support fails) (Li 2021). The magnitude of W_k determines the intensity of a rockburst. For a given amount of total released energy, the kinetic energy of the ejected rock mass (W_k) decreases with increasing energy dissipation by rock fracturing (W_f). The surface support elements, such as yieldable mesh (e.g., chain-link mesh) and mesh straps, can help accommodate a large amount of rock fracturing by increasing the energy dissipation in rock fracturing without support failure during rockbursts. Thus, the surface elements are an essential component of the ground support system in burst-prone areas.

For a ground support system in burst-prone areas, three main principles are well-acknowledged: use yielding support elements to increase energy absorption, address the weakest link, and establish an integrated support system (Kaiser et al. 1996; Hadjigeorgiou and Potvin 2007; Potvin et al. 2010; Li 2017b; Cai and Kaiser 2018; Wei et al. 2018; Kang et al.

2020; Pan et al. 2020b; Potvin and Hadjigeorgiou 2020; Qi et al. 2020).

Many studies have documented that yielding support is more effective than stiff support in burst-risk areas (Turner and Player 2000; Mazaira and Konicek 2015). Yielding support has been used worldwide to mitigate rockburst risks (Ortlepp 1968, 1992; Jager et al. 1990; Ortlepp and Stacey 1994). A yielding support system can accommodate a large amount of rock fracturing and absorb the associated dynamic energy (Cai and Kaiser 2018). This function can be achieved by yielding support elements (e.g., yielding rockbolts and mesh) with large deformation capacity.

It is well recognized that the weakest link of a support system is often the surface retaining elements and the connection between bolts and face plates (Kaiser and Cai 2012; Cai 2013; Potvin and Hadjigeorgiou 2020). It is highly likely the weak link in the support system can fail much earlier than before the reinforcements reach their theoretical design

Table 1 Failure mechanisms of ground support system observed from 254 rockburst damage events, after Heal (2010) and Potvin and Hadjigeorgiou (2020)

Failure mechanism	Percentage (%)
Surface support damage only, system survived	31
Rockbolt or cable ruptured, sheared or pulled out	30
Naked tendons, surface support failure only	19
Friction rock stabilizer ring failure	9
Surface fixture failure (plate punched through, nut stripped off, barrel and wedge failure)	6
Failure beyond embedment depth	5

capacity. Simser (2007) stressed that the ground failure often occurs with virtually intact rockbolts at rockburst sites, illustrating that the support failure is often around the collar area with tearing sharp-edged plate but non-breaking rebar. In this scenario, only part of the support capacity of rockbolts was achieved. Güler et al (2001) investigated the damage zone of rockbursts in South African gold mines, which found that 70% of rock ejection occurred due to failure of surface support elements while the rockbolts still remained intact. Also, as shown in Table 1, Heal (2010) studied 254 rockbursts in hard rock mines and concluded that only 30% of rockburst damage was due to the failure of reinforcement elements. In comparison, the majority of rockburst damage was caused by the failure of either the surface elements or the connection between the surface support and the reinforcements, highlighting the weakest link in a support system. Therefore, it is essential to identify the weakest link in a support system in burst-prone areas and replace it with a stronger one. For example, large face plates, of 350 mm × 300 mm and 3 mm thickness, were often adopted in burst-risk zones (Turner and Green 2005) to provide a wider cover area to prevent mesh from being torn off around the collar area. Adding rope lacing or steel straps to the mesh is also an effective approach to enhance the dynamic capacity of the weakest link (Ortlepp and Stacey 1998; Cai and Kaiser 2018).

In burst-prone areas, an integrated support system is effective when it can provide all the required support functions of reinforcement, retaining, holding and connection (Cai and Kaiser 2018). For example, a rockburst experiment in a South African mine demonstrated that the reinforcements alone cannot provide effective support when rockburst occurred (Milev 2005). In the experiment, the surface elements (mesh and lacing) were removed from the existing support system, and only the rockbolts remained in place. After the simulated rockburst (blasting), a 3.3 m/s of peak particle velocity (v_{pp}) and 2.5 m/s of ejection velocity were recorded. However, at the same time, the rockbolts remained intact, indicating that a limited portion of dynamic loading can exert on the rockbolts as the support system missed

an essential component of the load transfer elements (e.g., plates and mesh) (Ortlepp 2006). Furthermore, for rockburst conditions, Villaescusa et al (2016) stressed that the larger the size of loosened blocks, the more reinforcement action is required to absorb energy and stabilize the blocks. In contrast, small loosened blocks need surface support elements, such as mesh, shotcrete and/or their combination. The combination of rockbolts and surface elements can help to increase the support performance (Ortlepp and Stacey 1994; Cai 2013). The integrated system can effectively redistribute the dynamic loading more evenly and allow the rockbolts to withstand more loading, as verified in practical cases described by Milev (2005).

In general, the most important aspect of an integrated support system is to ensure the deformation compatibility between each support element within the system (Cai and Kaiser 2018). Then, the support system can reach the highest possible dynamic support capacity, instead of failing at the weakest link before the yielding rockbolts have even reached their yielding state.

3 Support capacities of ground support elements in the laboratory

3.1 Dynamic test approaches for support elements

In the laboratory, two dynamic testing methods are commonly used to assess the support capacities of ground support elements: free-fall of a mass and momentum transfer (Li 2017b). For the free-fall method, dynamic loading is simulated by directly dropping a mass over a certain height onto the support element. The load and the displacement of the tested element are recorded by a load cell under the impact plate and a differential extensometer, respectively. The support capacities of the tested elements can then be assessed. The set-up of the free-fall method was originally designed at CANMET Mining in Canada. Similar set-ups have also been constructed in Australia, South Africa and Europe. For the

Table 2 Characteristics of three representative dynamic testing facilities

Item	WASM	Geobrugg	CANMET
Location	Kalgoorlie, Australia	Walenstadt, Switzerland	GRC, Canada
Test elements	Mesh; Mesh and bolt	Mesh, bolt and shotcrete	Bolt
Loading mode	Momentum transfer	Mass free-fall	Mass free-fall
Number of tested bolts	none/1	4	1
Size of mesh (m × m)	1.3 × 1.3	3.6 × 3.6	N/A
Maximum drop weight (kg)	4500	9640	3000
Maximum drop height (m)	6	4.9	2
Maximum impact velocity (m/s)	10.8	9.8	6.3
Maximum impact energy (kJ)	264	463	58.9

momentum transfer approach, the rockbolt is installed in a split tube attached to a known mass. This set-up is fixed on a holding beam. The whole arrangement is then dropped to buffers on the ground. The potential energy of the dropping mass is transferred to the rockbolts when the holding beam impacts the buffers. This dropping test approach is adopted by the Western Australia School of Mines (WASM) (Player et al. 2004; Villaescusa et al. 2013; Li 2017b).

Currently, three representative dynamic test facilities are commercially active worldwide: CANMET, WASM, and Geobrigg. Their testing capacities and characteristics are summarised in Table 2. As the set-ups differ significantly among dropping test facilities, it is essential to provide the testing procedures and input parameters (e.g., dropping mass and height) when reporting the testing results for support elements (Cai and Kaiser 2018; Li et al. 2021).

3.2 Yielding rockbolts

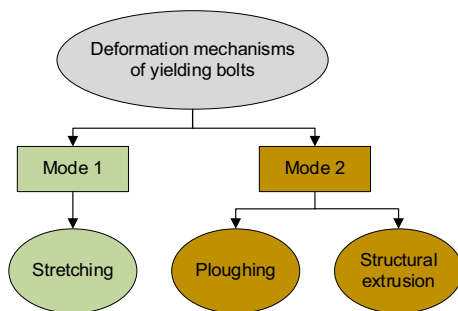


Fig. 4 Classification of support mechanisms of yielding rockbolts (Sharifzadeh et al. 2020)

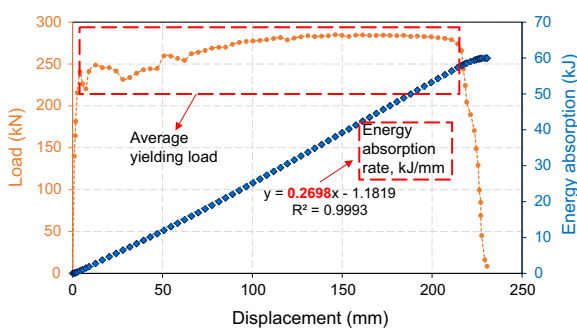


Fig. 5 Dynamic test of D-bolt with 22 mm diameter, redrawn after Li and Doucet (2012)

According to the energy-absorbing mechanisms, yielding rockbolts can be classified into two categories (Hao et al. 2020; Sharifzadeh et al. 2020): stretching rockbolts, and ploughing or structural extrusion rockbolts, as shown in

Fig. 4. The stretching rockbolts can elongate with bulking rock mass and absorb energies through plastic deformation of the bolt shank. The ploughing or structural extrusion rockbolts absorb energies by ploughing of the anchor in the grout or extrusion of the shank within the pre-designed structural elements (e.g., expandable sleeves).

As an example, the support performance of D-bolts in a dynamic loading test is shown in Fig. 5. Li and Doucet (2012) tested D-bolts using the dynamic testing facility at CANMET. A D-bolt with 22 mm diameter and 1.5 m of test section can elongate approximately 220 mm and absorb 60 kJ of energy, as shown in Fig. 5. The total energy absorption is calculated by the integral area between the load–displacement curve and the displacement axis. The average yielding load on the D-bolt can be determined to be approximately 265 kN. Sharifzadeh et al. (2020) proposed that the slope of the linear regression of the energy absorption can reflect the energy absorption capacity of a specific yielding bolt, which is defined as the energy absorption rate (EAR) with a unit of kJ/mm. The EAR of the D-bolt is approximately 0.269 kJ/mm, as shown in Fig. 5. Furthermore, the unit of EAR is dimensionally the same as load (kN), indicating that the two terms can be converted to each other. For example, 0.269 kJ/mm is equivalent to 269 kN. After this conversion, it was found that the EAR is an approximation of the average yielding load (Sharifzadeh et al. 2020). The initial stiffness of a rockbolt refers to the slope of the secant line from the origin point to the first peak point in the load–displacement curve (Li 2021). For example, the initial stiffness of the D-bolt shown in Fig. 5 is approximately 22.28 kN/mm. The initial stiffness is an important indicator to assess the support capacity of rockbolts, as rockbolts with high stiffness are required in burst-prone areas to effectively restrain rock bulking (Li 2021).

A number of widely used and recently developed yielding rockbolts have been investigated, and their support capacities are summarised in Table 3.

Some yielding rockbolts, including the cone bolt, Dura-bar, Garford and Hao-bolt, have initial stiffness of less than 5 kN/mm, indicating low stiffness performance when rock bulking occurs. This can cause concern in burst-prone areas, as large deformation can occur due to the low stiffness support in a high-stress environment (Li 2021). In comparison, the 20MnSi rockbolts and BHRB400 rockbolts have outstanding performance on the initial stiffness, probably because of the high strength metal material used for the rockbolts. Generally, the stretching rockbolts have relatively higher initial stiffness (> 10 kN/mm in general) than the ploughing or extrusion rockbolts. Nevertheless, it is more reasonable to compare the initial stiffness of different rockbolts tested in the same testing facility than in different facilities because the initial stiffness of the same rockbolt samples can vary considerably in different testing facilities,

Table 3 Summary of the support capacities of yielding rockbolts

Bolt	Type	Initial stiffness (kN/mm)	Deformation (mm)	Energy absorption (kJ)	Average yielding load (kN)	Energy absorption rate (kJ/mm)	Data source
Cone bolt	ploughing	3.28	300	60	196	0.183	Player et al. (2008)
Modified cone bolt (MCB)	ploughing	–	250	20	150	0.16	Sharifzadeh et al. (2020)
Yield-Lok	ploughing	11.50	177	17	80	0.077	Wu and Oldsen (2010)
Durabar	ploughing	3.25	600	48	80	0.083	Li (2017b)
Garford bolt	extrusion	4.01	400	50	108	0.183	Player et al. (2008)
Roofex	extrusion	8.40	275	22	60	0.059	Charette and Plouffe (2007)
He-bolt	extrusion	9.99	925	145.6	168	0.158	He et al. (2014)
Hao-bolt	extrusion	2.83	309	41	145	0.141	Hao et al. (2020)
Wang-bolt	extrusion	14.75	158	40	264	0.262	Wang et al. (2013)
D-bolt	stretch	22.28	218	60	265	0.27	Li (2012), Li and Doucet (2012)
MP1 bolt	stretch	9.40	174	47.8	285	0.279	Sharifzadeh et al. (2020)
PAR1 bolt	stretch	10.89	230	45.6	225	0.205	NCM (2019), Sharifzadeh et al. (2020)
20MnSi Rebar	stretch	69.93	328	62.8	204	0.197	Wang et al. (2018)
BHRB400	stretch	46.36	384	77	220	0.208	Wang et al. (2018)
AIEA-T	stretch	14.50	330	42	120	0.127	Dai et al. (2020)

Table 4 Typical demand for ground support design and yielding bolts selection, updated after Sharifzadeh et al. (2020)

Ground demand category	Demand for ground support (Villaescusa et al. 2015)			Bolt selection
	Reaction pressure (kPa)	Surface displacement (mm)	Energy absorption (kJ/m ²)	
Low	< 100	< 50	< 5	Yield-Lok, Durabar, Roofex
Medium	100–150	50–100	5–15	Garford, Hao-bolt
High	150–200	100–200	15–25	Cone bolt, MCB, He-bolt
Very high	200–400	200–300	25–35	D-bolt, MP1 bolt, PAR1, 20MnSi Rebar, BHRB400
Extremely high	> 400	> 300	> 35	N/A

while the initial stiffness (for the same rockbolts) changes little in the same facility (Li et al. 2021).

Villaescusa et al (2015) summarized the typical rock mass demand for ground support elements in burst-prone areas, as shown in Table 4. For the representative case of bolting density one bolt per square metre of face, the average yielding load in Table 3 can be regarded as the load on the excavation surface per unit area, which is equivalent to the reaction pressure in Table 4. Furthermore, the energy absorption rate (EAR) and average yielding load (i.e., reaction pressure) can reflect the ‘yielding stiffness’ of the yielding rockbolts. The magnitudes of the two terms are approximately equal to each other. Thus, the reaction pressure can be used as a primary indicator in yielding rockbolts classification.

As shown in Fig. 6, the yielding rockbolts are classified into low, medium, high and very high according to the ground support demand proposed by Villaescusa et al

(2015). Although all the yielding rockbolts have more than 15 kJ of energy absorption capacity, a high level of energy absorption demand, the reaction pressure differs in a wide range of 60 kPa (Yield-Lok) to 285 kPa (MP1 bolt).

It is of interest that all the yielding rockbolts of stretching type are identified in the ‘very high’ category, indicating that the stretching shank can absorb ‘very high’ seismic energy and produce ‘very high’ reaction pressure during the yielding deformation of the bolt. In comparison, the ploughing yielding bolts (including ploughing and structural extrusion) have various levels of reaction pressure, and only the Wang-bolt has a ‘very high’ level of reaction pressure. In addition, as shown in Table 3, the ploughing bolts have relatively ‘weaker’ initial stiffness compared to that of stretching bolts. The classification generally reflects that the ploughing elements and/or the structural extrusion devices do not have a stable performance regarding the resisting force (i.e.,

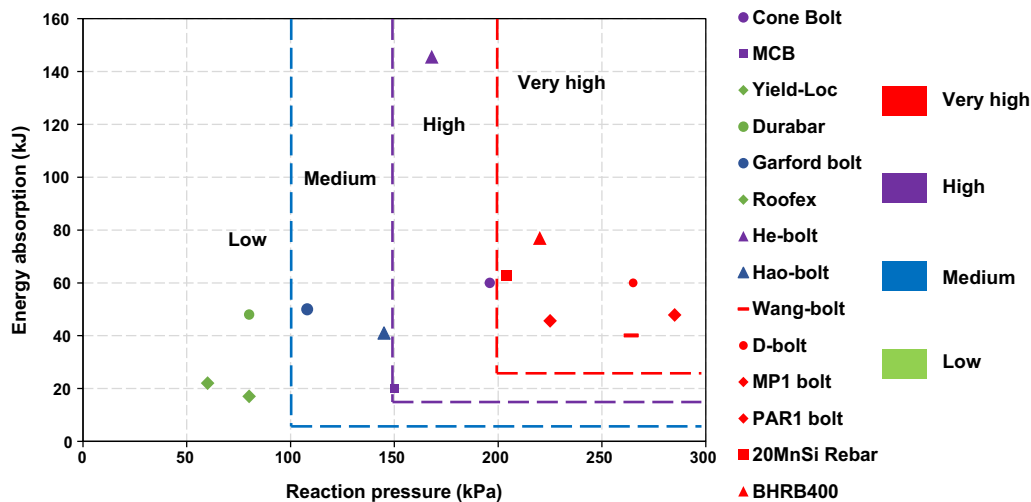


Fig. 6 Classification of yielding bolts based on energy absorption and reaction pressure capacity listed in Table 3

reaction pressure) generated during the process of accommodating dynamic rock bulking. Nevertheless, Kaiser et al. (1996) suggested that it would be suitable for reinforcements in burst-prone areas when the reinforcements can provide up to 300 mm of accommodation displacement and load capacity of greater than 100 kN. With the development of yielding reinforcements in recent decades, many yielding rockbolts can meet this requirement.

3.3 Support capacities of integrated support systems

Surface support elements have been tested using the drop test approach by numerous studies (Kaiser et al. 1996; Ortlepp and Stacey 1998; Stacey and Ortlepp 2001; Brändle et al. 2017). The majority of the tests connect the surface support elements (mainly the mesh) and rockbolts together as an integrated support system. The drop tests are mainly conducted in South Africa (Ortlepp and Stacey 1998; Stacey and Ortlepp 2001), CANMET GRC in Canada (Kaiser et al. 1996; Cai and Kaiser 2018), Geobruigg in Switzerland (Bucher et al. 2013; Brändle et al. 2017) and WASM in Australia (Villaescusa et al. 2015). However, for dynamic tests in South Africa and GRC, only the total input energy (i.e., impact energy) can be determined using dropping mass and dropping height. The portion of energy absorbed by each element in the support system cannot be explicitly evaluated. In comparison, the more recently developed test facilities at Geobruigg and WASM can directly assess the energy absorption capacity of each support element within a tested system.

3.3.1 Dynamic test results in South Africa and GRC

The testing facility in South Africa used four rockbolts with a 1 m spacing of bolt pattern to restrain the surface support elements (Stacey and Ortlepp 2001). Various surface support elements were tested in the facility, including mesh, shotcrete, rope lacing, and their combinations. The size of the surface support sample was 1.6 m × 1.6 m. Three layers of concrete blocks (250 mm × 250 mm × 100 mm) were laid onto the surface support elements to simulate the attached ‘rock mass’. The impact load was produced by dropping the loading mass onto a 40 mm thick steel impact plate. Thus, the dynamic load was applied uniformly by transferring load through the steel plate and concrete blocks to the surface support elements. During the impact loading process, a significant part of the impact energy was dissipated by crushing the stacked concrete blocks, and a small amount (unknown) of impact energy transferred to the tested surface support elements (Potvin and Hadjigeorgiou 2020). Two drop weights (1050 and 2700 kg, respectively) were used. The maximum impact velocity can reach up to 8.1 m/s, which corresponds to 3.3 m of dropping height and 70 kJ of maximum impact energy.

In GRC tests, the impact load was applied directly as a point load in the center of the surface support component. The loading mass in the GRC facility was 565 kg with a range of impact velocities from 4.4 m/s to 7.7 m/s. The maximum impact energy was 16.6 kJ (Cai and Kaiser 2018). The mesh sample was restrained by four stiff rockbolts with 0.85 m spacing of diamond pattern. Of note is that the direct loading mode in GRC was different from the loading mode in South Africa, where the loading mass was dropped onto the stacked concrete blocks laid on the mesh to generate indirect impact loading on the mesh sample. Cai and Kaiser

(2018) argued that the point loading mode in GRC may be more representative of rockbursts than the distributed loading mode in South Africa, as the distributed loading mode in South Africa over-uniform the stress exerted on surface samples in an actual rockburst scenario.

Cai and Kaiser (2018) compared the energy absorption capacities of various support elements by compiling the test results together based on their tested bolt pattern in GRC. In comparison, Martínez et al (2020) normalized the test results based on the mesh size used in the test facilities. Furthermore, the test configurations vary remarkably between the testing facilities at GRC, Geobruigg and WASM. Thus, it is hard to have a clear trend of comparison for the support

elements tested in different configurations. Fig. 7 summarises the test results of various support elements in South Africa and GRC. The test results are normalized according to the bolt pattern used to restrain the surface elements, which is consistent with the comparison method used by Cai and Kaiser (2018).

The loading test results showed that the un-reinforced shotcrete and fiber-reinforced shotcrete had the poorest performance as they can resist approx. < 10 kJ/m² of impact energy and < 50 mm of deflection. Most weldmesh support systems cannot resist more than 10 kJ/m² of impact energy, and the central deflection of the weldmesh was approximately 100 mm. The chain-link mesh support

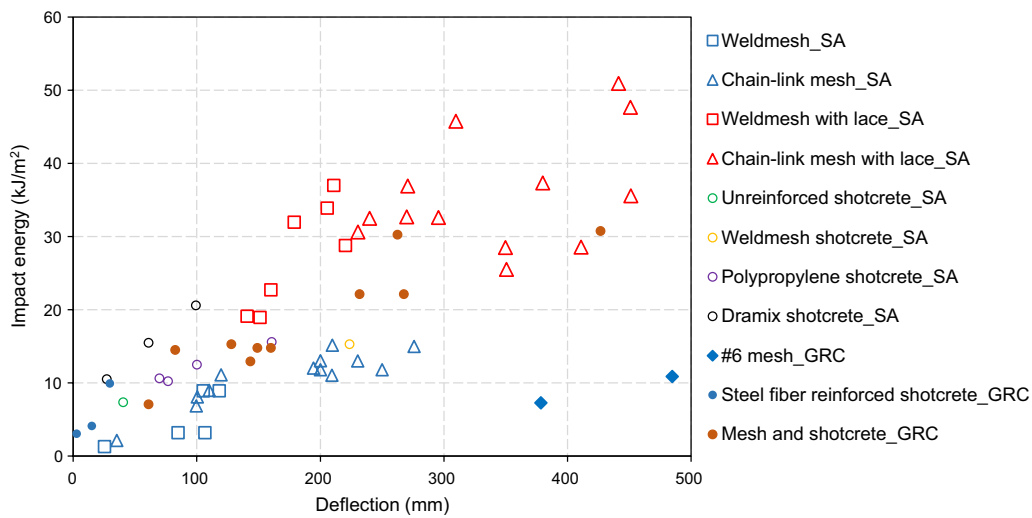


Fig. 7 Performance of various surface support elements, updated from Stacey and Ortlepp (2001); Cai and Kaiser (2018). Note: SA means the support elements were tested in South Africa (with unfilled

symbols). GRC means the support elements were tested at CANMET GRC in Canada (with filled symbols)

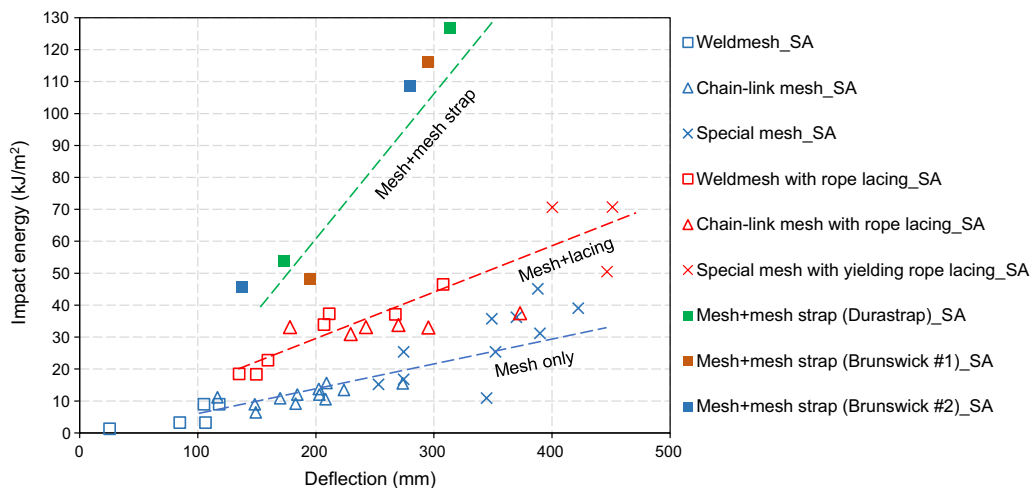


Fig. 8 Enhancement of mesh performance by adding rope lacing and mesh strap, redrawn after Cai and Kaiser (2018). Note: special mesh refers to yield meshes that were commercially available in South Africa

systems had better performance than the weldmesh support systems.

In South Africa, Stacey and Ortlepp (2001) and Kuijpers et al (2002) found that adding rope lacing and mesh strap to mesh elements can substantially enhance the support performance of the support system. The capacity of the mesh support system was approximately doubled by adding rope lace, and it was four times higher when adding mesh straps, as shown in Fig. 8. The rope lacing and mesh straps can reduce the mesh deflection between rockbolts to enhance the support capacity of the integrated system, which is similar to reducing the bolt spacing in the support system (Cai and Kaiser 2018).

3.3.2 Dynamic test results at Geobruigg and WASM

For the Geobruigg test facility in Switzerland, the size of the mesh sample is 3.6 m × 3.6 m. Four yielding bolts are used to restrain the mesh element with a typical bolt pattern (1.2 m × 1.2 m). Bucher et al (2013) conducted drop tests on a support system consisting of TECCO G80/4 chain-link mesh and four D-bolts. The D-bolts had a diameter of 20 mm, bolt length of 3 m and deformable section of 1.5 m, indicating 225 mm of possible elongation by assuming 15% of ultimate strain. The loading mass in this test was 6280 kg, and the loading height was 3.25 m. Thus, the impact energy was approximately 200 kJ. The mesh sample was installed within two concrete slabs of different thicknesses to simulate two types of rock mass conditions. A thicker concrete slab represented stiff rock mass, and a thinner concrete slab represented softer rock mass condition. The test results are shown in Table 5.

For the two drop tests, the test facility dissipated most of the impact energy (approximately 80% of the total input energy). Although there was no remarkable difference for the total energy absorbed by the support system between the stiff set-up (i.e., thicker concrete slab) and soft set-up (i.e., thinner concrete slab), the distribution of energy absorption between the reinforcements and mesh elements differed significantly. For a stiff rock mass environment, the reinforcements took approximately 75% of the total energy absorbed by the support system, while the mesh element only took 25% of the total absorbed energy. In contrast, for a soft rock mass environment, the reinforcements dissipated

a small portion (30%) of the total absorbed energy, while the mesh element dissipated the majority (70%) of the energy. It highlighted that the stiffness of the supported rock mass can significantly influence the distribution of energy absorption between reinforcements and mesh elements during rockbursts. Furthermore, the test results generated debate on whether rockbursts are better represented by the stiff set-up or the soft set-up in testing (Potvin and Hadjigeorgiou 2020). The stiff set-up can represent a relatively intact rock mass condition around excavations before the rockburst. In contrast, the soft set-up can represent a relatively fractured rock mass condition. The soft set-up may better represent the rock mass condition in deep coal excavations, as the coal mass is usually in failure around the deep excavations due to the low strength of the coal. It is also probable that both stiff and soft rock mass conditions can occur in different rockbursts in the same mine site.

As shown in Fig. 9b, at WASM, a single rockbolt is placed through the drop beam, loading mass (i.e., the loading rings) and curved plate. The frame is then fixed onto the drop beam with load cells. The curved plate is placed in the central position of the mesh sample. The size of the mesh sample is 1.3 m × 1.3 m. According to the testing configuration, the WASM facility can test only part of a ground support system (Cai and Kaiser 2018), as the single rockbolt at

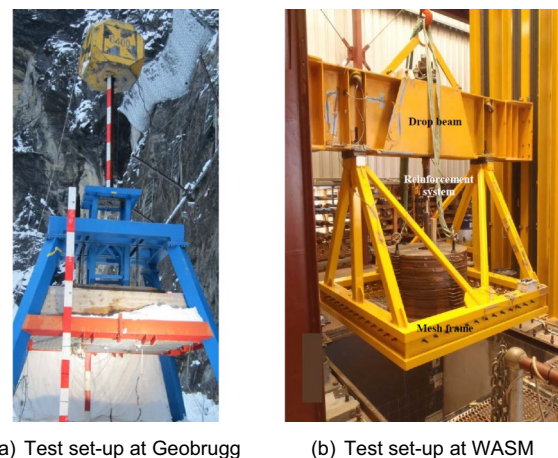


Fig. 9 Configuration of the drop test facility at Geobruigg and WASM (Bucher et al. 2013; Villaescusa et al. 2015)

Table 5 Drop test results of support system at Geobruigg (Bucher et al. 2013)

Tested rock type	Mesh deflection (mm)	Bolt deform (mm)	Energy absorbed by mesh (kJ)	Energy absorbed by bolts (kJ)	Total energy absorbed by support system (kJ)	Energy absorbed by test rig (kJ)
Stiff	140	150	10	32	42	158
Soft	300	25	26	10	36	164

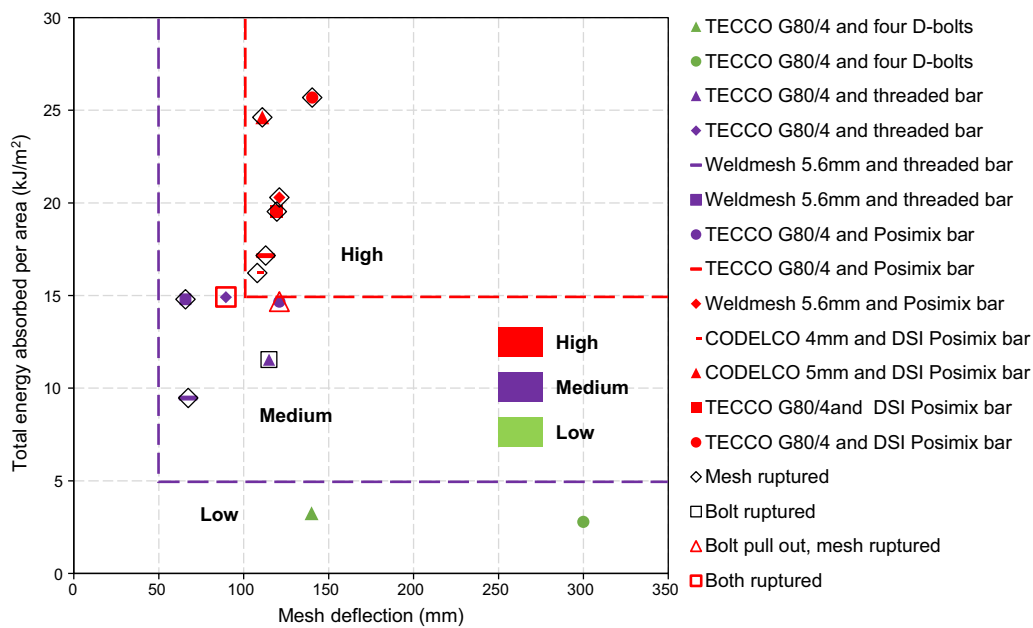


Fig. 10 Classification of ground support systems based on energy absorption and mesh deflection capacity. Note: the first two support systems (TECCO G80/4 and four D-bolts) were tested at Geobrugg, and the rest of the support systems were tested at WASM

WASM cannot fully represent a complete bolting pattern which needs four rockbolts.

Figure 10 summarises the dynamic test results of ground support systems at Geobrugg and WASM. The support systems can be classified into low, medium and high support capacities according to the support demand proposed by Villaescusa et al (2015) in Table 4. The two support systems tested at Geobrugg are classified as low support capacity. However, no ruptures occurred on the main support elements (i.e., the four D-bolts and the mesh) after the drop tests, indicating that the two tested support systems did not reach their maximum support capacity at Geobrugg. In contrast, all the 11 support systems tested at WASM reached their maximum support capacity as ruptures occurred on either part (reinforcements or mesh elements) or all of the support systems after the drop tests.

Based on Fig. 10, almost all the support systems with chain-link mesh and yielding rockbolts (i.e., decoupled rockbolts) were classified as high support capacity (greater than 15 kJ/m² of energy absorption and 100 mm of mesh deflection). All the support systems with chain-link mesh and stiff rockbolt (i.e., thread rebar) were classified as medium support capacity. Support systems had medium support capacity when the system used weldmesh and stiff rockbolts. In comparison, a support system may reach high support capacity when the system used weldmesh and yielding rockbolts (i.e., the support system with weldmesh and decoupled Posimix rebar). Except for the support system tested in the soft set-up at Geobrugg, the energy absorbed by surface support elements (i.e., mesh) was less

than 10 kJ before the systems failed, with the mesh rupturing in most cases. Furthermore, drop tests pointed out that the ground support system often fails on the weakest link, which is usually the surface support elements. Thus, the capacity of a ground support system can be conservatively assessed by the capacity of the mesh in the system (Potvin et al. 2010). It also stressed that low support performance can be expected when a support system uses high capacity yielding reinforcements but low capacity surface support elements. In this scenario, minimal load is transferred to the reinforcements due to premature failure of the surface support elements.

In general, it is essential to improve the capacity of surface support elements to enable the load to be transferred between the reinforcements and the mesh without premature failure in mesh elements. As such, the energy can be dissipated through both the reinforcement elongation and the mesh deflection.

3.4 Interpretation of support capacities obtained from drop tests

Interpretation of drop test results is necessary when applying the tested support systems in practice (Potvin et al. 2010), as certain limitations exist in the drop tests. For example, the drop test approach does not consider the interaction between the ground support system and the supported rock mass. Different supporting environments may significantly change the distribution of energy dissipation of support elements in a support system, as demonstrated by the test results at

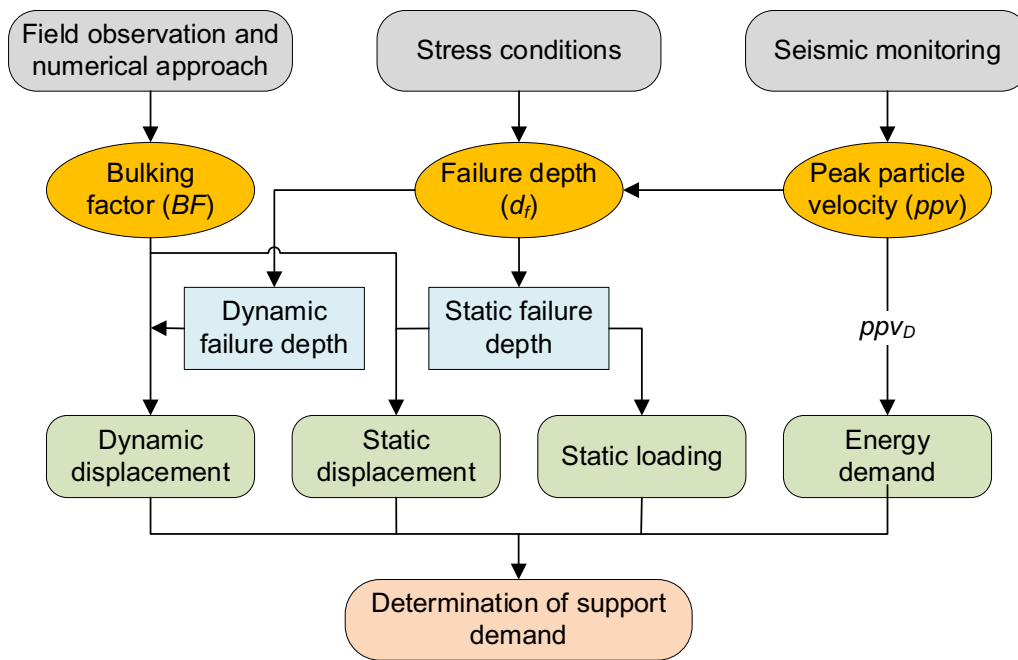


Fig. 11 Flowchart of support design using CRH approach

Geobrigg. Also, the test protocols can have considerable impacts on the test results (Potvin et al. 2010). It is essential to recognize the differences in various testing facilities when interpreting and compiling their test results. Different testing facilities have different testing characteristics, such as the loading modes, mesh size, number and bolt pattern of rockbolts, and boundary conditions used in the facilities. Furthermore, the support capacities in the drop tests are determined based on an idealized dynamic tensile loading mode, especially for the tested reinforcement elements. The load transfer and failure mode of the support system can be different when significant dynamic shearing load exerts on the support elements during rockbursts. In this scenario (i.e., shearing load), some of the arguments concluded from the drop tests may be invalidated. In addition, the support performance can be different when the installation quality and loading mechanism (e.g., strain burst and fault-slip burst) change at a particular mine site (Player et al. 2008).

All testing approaches can help assess support capacity of support elements. The critical part is to link the test results from various testing techniques and apply the test results in practice. Nevertheless, it would be beneficial to develop standard testing procedures across testing facilities (Potvin and Hadjigeorgiou 2020).

4 Engineering practice of ground support systems in burst-prone mines

This section summarises the international best-practice ground support systems used in burst-prone mines. It aims to provide insights into control strategies that can be adopted in burst-prone coal mines.

4.1 Canadian rockburst handbook (CRH) approach

The method used in CRH is a semi-analytical based approach to assess the support demand in dynamic ground conditions (Kaiser et al. 1996; Kaiser and Cai 2012; Cai 2013; Cai and Kaiser 2018). The support demand is determined according to the demand assessment of static loading, static displacement, dynamic displacement and energy release in burst-prone areas, as shown in Fig. 11.

The depth of failure around excavations can be estimated using a semi-empirical relationship between the failure depth and the stress conditions around the excavations, as given by Eq. (1). Then, the static loading approximately equals the deadweight of the failure zone. Of note is that Eq. (1) and its parameters are obtained using a database of tunnels in a relatively stiff mining environment in hard rock mines (Kaiser and Cai 2013). Therefore, for excavations in relatively soft rock such as coal in a soft loading environment, it is reasonable to expect considerably larger failure depth around the excavations.

$$\frac{d_f}{a} = C_1 \frac{\sigma_{\max}}{\sigma_c} - C_2 = C_1 SL - C_2 \tag{1}$$

$$a = \frac{L}{\sqrt{2}} \tag{2}$$

$$SL = \frac{\sigma_{\max}}{UCS} \tag{3}$$

where, d_f is the depth of failure; a is the equivalent opening radius; L is the shortest roadway dimension between height or width; C_1 and C_2 are two constants. For static conditions, the average values of C_1 and C_2 are 1.37 and 0.57, respectively. For dynamic ground conditions, C_1 and C_2 are determined based on peak particle velocity around excavations (Kaiser 2006). σ_c is the uniaxial compressive strength (UCS). SL refers to the stress level around excavations, σ_{\max} is the maximum stress at the excavation boundary.

The bulking factor (BF) refers to the change of unidirectional length when the stress-driven failure occurs. The support displacement demand (static and dynamic) can be assessed by multiplying the failure depth (d_f) by the BF , as given by Eq. (5).

$$BF = \frac{d_1}{l}; \text{ if } l = d_f \text{ then } BF_{d_f} = \frac{d_1}{d_f} \tag{4}$$

$$\frac{u_{\text{wall}}}{a} = BF(C_1 SL - C_2) = BF \frac{d_f}{a} \tag{5}$$

where, d_1 is the length change that is perpendicular to the excavation boundary; l is the original length; the bulking factor (BF) varies from approximately 1% to 50% according to field observation and numerical modeling (Kaiser and Cai 2013); u_{wall} is the wall displacement.

For a rockburst event, the kinetic energy of the ejected rock is related to the peak particle velocity (ppv). In practice, the design ground motion (ppv_D), rather than ppv, is often used for the estimation of kinetic energy demand in the support system, as the ppv_D is an approximation of the upper bound of the possible magnitudes of ppv (Kaiser and Cai 2013; Potvin and Hadjigeorgiou 2020). The ppv_D can be estimated using a semi-empirical scaling law given by Eq. (6). Of note is that this scaling law assumes the seismic source as a point source and the seismic wave propagates in a spherical pattern rather than the actual complex radiation pattern produced by a slip event. Therefore, the spherical assumption is conservative, and it does not consider the impacts of the shear slip orientation on the magnitude of traveling seismic stress waves and seismic energy.

$$\text{ppv}_D = \frac{C \times 10^{\frac{1}{2}(M_R+1.5)}}{R} \tag{6}$$

where, M_R is the Richter magnitude of the seismic event; R is the distance between the seismic source and the target areas; C is an empirical constant considering reliability and static stress drop.

The total energy of the ejected rock mass mainly consists of kinetic energy and potential energy, as given by Eq. (7). The energy absorption capacity of the support system should be greater than the total energy.

$$E_{\text{total}} = \frac{1}{2}mv_e^2 + mgd_s \tag{7}$$

where, v_e is the ejection velocity; m is the mass of ejected rock; d_s is the deformation exerted on the support system; g is gravitational acceleration. Of note is that the potential energy term is only taken into account if d_s points vertically downwards.

Although the ppv or ppv_D can be used to estimate the kinetic energy demand for the support system (Kaiser et al. 1996; Kaiser and Cai 2012; Zhang et al. 2015), the ejection velocity (v_e) is different from the ppv or ppv_D. Some factors, such as the interaction of ground motion and support system, the evolution of ppv around the excavation, the influence of loading stiffness of local environment and the involvement of strain energy within country rock, are extremely complex. As a result, there may be no direct relationship between ppv and ejection velocity (Kaiser and Cai 2013). Therefore, the accurate energy absorption capacity for a support system still needs much more research (Potvin and Wesseloo 2013; Wei et al. 2018).

4.2 The Western Australian School of Mines (WASM) approach

As discussed in Sect. 3, researchers at WASM have established a substantial database for the dynamic capacity of both individual support elements and integrated support systems. WASM also conducted experiments in the laboratory and field to assess the ground support demand in burst-prone conditions. In general, the support energy demand for a burst-prone area is mainly related to the amount of mass that would be ejected and the velocity of the ejected mass (Villaescusa et al. 2016).

Villaescusa et al (2016) postulated that the UCS of the country rock of excavations may be the most reliable index to assess the ejection velocity, as the kinetic energy of the ejected rock mass is dominantly controlled by the strain energy stored behind the excavation ribs. Kusui et al (2016) conducted a series of scaled-down experiments of circular excavations (200 mm diameter) in hard rock, demonstrating that the ejection velocity approximately increased linearly

with increasing UCS of intact rock. The ejection velocity ranged from 2 to 10 m/s for various rock types, which can be validated against the ejection velocity observed in actual rockburst in hard rock mines (Ortlepp 1993; Drover and Villaescusa 2015, 2016).

Villaescusa et al (2016) classified the failure mechanisms of burst damage zone into spalling failure and structurally controlled failure. For rockbursts in hard rock mines, the majority of damaged areas are characterized by spalling failure, where tensile fracturing of rock (associated with ejection of rock slabs) occurs sub-parallel to the excavation surface. In this scenario, the failure depth is shallow and often ranges from 0.25 to 0.5 m, corresponding to approximately 0.6 t/m² to 1.3 t/m² for hard rocks. The spalling failure depth gradually decreases with increasing rock strength (Villaescusa et al. 2016). The energy demand is often within 20 kJ/m² for a support system in spalling failure conditions. For structurally controlled failure, the failure depth may exceed 2 m, and large loosened blocks can be ejected along the major structures. The ejected mass can exceed 1.5 t/m², and the corresponding support energy demand is often greater than 25 kJ/m². In extreme conditions, the support energy demand can be greater than 60 to 80 kJ/m² (Drover and Villaescusa 2016).

After determining the energy demand in burst-prone areas, the support system can be selected according to the support capacity obtained from drop tests. The capacities, including the force, deformation and energy absorption, of the selected support system should be greater than the rock mass demand in burst-prone areas.

4.3 Rockburst damage potential approach

As discussed above, certain limitations exist when determining ground support demand in burst-prone areas using analytical and laboratory test approaches. Alternatively, numerous studies have assessed the support performance of various ground support systems in dynamic ground conditions, aiming to provide empirical guidance in ground support selection (Heal et al. 2006; Potvin 2009; Mikula 2012; Duan et al. 2015a; NGI 2015; Morissette and Hadjigeorgiou 2019). As an example, the rockburst damage potential (RDP) approach proposed by Heal et al (2006) is one of the empirical-based approaches to determine the ground support systems in dynamic ground conditions. The RDP is highly related to the excavation vulnerability potential (EVP) and the ppv produced by a given seismic event. This relationship was validated by a database consisting of 254 damage zones and 80 rockburst case histories in hard rock mines in Australia and Canada.

Excavation vulnerability potential (EVP) is established empirically to quantify the influence of local site conditions on damage potential around excavations. The EVP is

assessed by five major factors given by Eq. (8): static stress conditions ($E1$), the capacity of the ground support system ($E2$), excavation span ($E3$), geological structure condition ($E4$), and roadway orientation condition ($E5$). The damage potential of excavations increases with increasing EVP.

$$EVP = \frac{E1}{E2} \times \frac{E3}{E4} \times E5 \quad (8)$$

The static stress condition $E1$ is expressed by the ratio of static loading to intact rock strength, as given by Eq. (9).

$$E1 = 100 \times \frac{\sigma_{1M}}{UCS} \quad (9)$$

where, σ_{1M} is the maximum principal stress around excavations.

Ground support systems are rated in five levels according to their general support capacities ($E2$). Users need to determine the levels of their local support system according to the empirical rating scheme. The excavation span factor ($E3$) directly equals the diameter (metre of unit) of the maximum circle that can be inserted into the excavation. The geological structure condition ($E4$) considers the geological discontinuities and ground conditions in the target area. Turcotte (2014) added the roadway orientation factor ($E5$) to the calculation of EVP, as the relative orientation of roadway to the foliation had considerable impacts on the excavation stability (Mercier-Langevin and Hadjigeorgiou 2011).

Heal et al (2006) proposed a rating scheme for the rockburst damage scale (RDS), which is a modified version of the RDS proposed by Kaiser et al (1992). The RDS proposed by Heal et al (2006) classified the damage conditions into five levels, as shown in Table 6, which was applied to the rockburst cases (i.e., the 254 damage zones and 80 rockburst case histories).

It was found that the rockburst damage scale (RDS) of the 254 damage zones had a strong correlation with the corresponding values of EVP and peak particle velocity

Table 6 Rockburst damage scale (RDS) classification (Heal et al. 2006)

Rockburst damage scale	Rock mass damage	Support damage
R1	No damage, minor loose	No damage
R2	Minor damage, less than 1 tonne displaced	Support system is loaded, loose in mesh, plates deformed
R3	1–10 tonnes displaced	Some broken bolts
R4	10–100 tonnes displaced	Major damage to support system
R5	> 100 tonnes displaced	Complete failure of support system

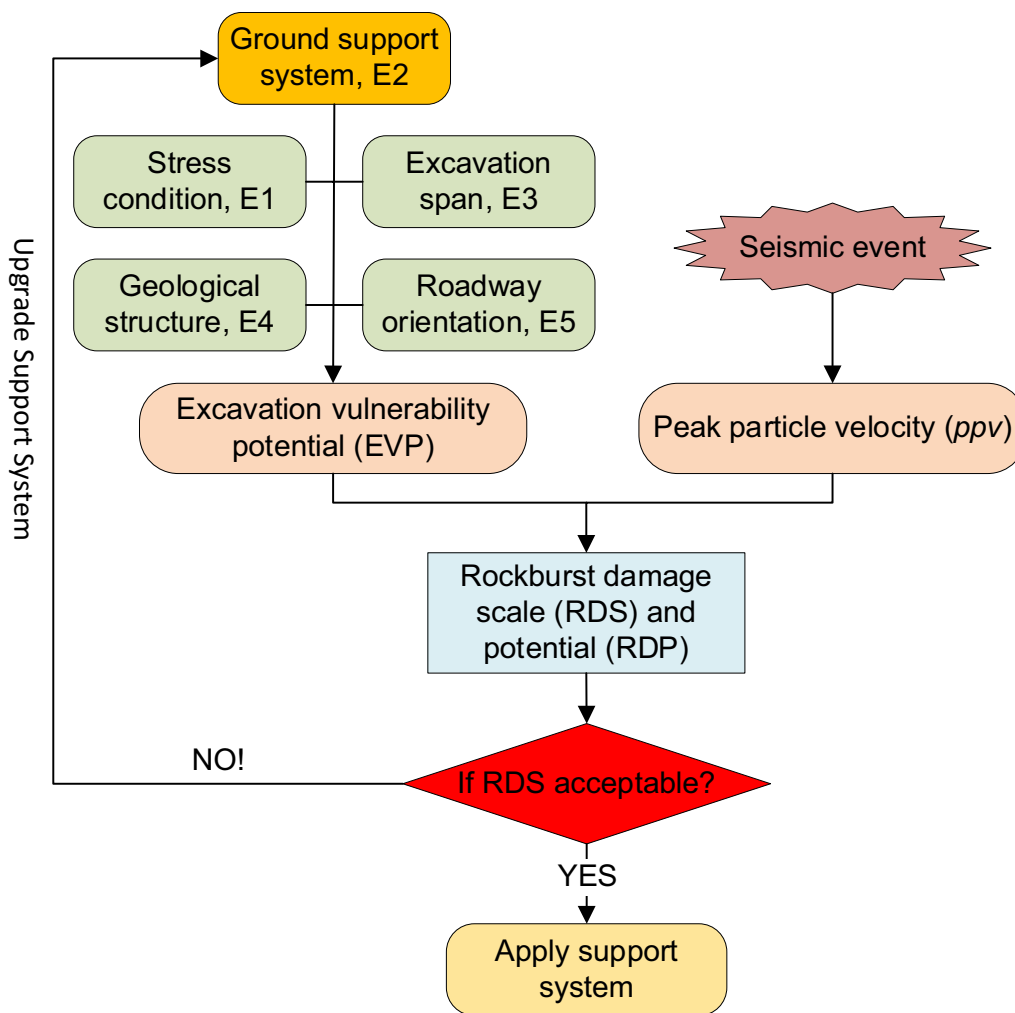


Fig. 12 Flowchart of support design using rock burst potential (RDP) approach

(ppv). The ppv of a given seismic event is estimated by Eq. (10). Then, the rock damage potential (RDP) was proposed according to the empirical relationship between the $EVP \times ppv$ and the RDS, which can be used as a design tool for ground support system selection in burst-prone mines. For example, for a given seismic event, the generated ppv can be estimated using Eq. (10) for any target areas in sites. Then, as the factors of $E1$, $E3$, $E4$ and $E5$ of the target area are constant, the required capacity of support system (i.e., $E2$) can be determined by adjusting the RDS to an acceptable level, i.e., R1 or R2 in general (Potvin and Hadjigeorgiou 2020), as shown in Fig. 12.

$$ppv = \frac{1.4 \times 10^{(M_R/2)}}{R} \tag{10}$$

where, M_R is the Richter magnitude of the seismic event.

The RDP map is a real-time assessment for the RDS, as the ppv and stress condition ($E1$) change during excavations. The real-time RDP can highlight the areas that have burst-prone risks, and the support system at the target zone can be upgraded accordingly (Potvin and Hadjigeorgiou 2020). The RDP approach has been applied in numerous studies (Hudyma and Potvin 2010; Turcotte 2014; Duan et al. 2015b), although certain limitations exist. For example, Kaiser and Cai (2013) pointed out that the EVP index does not capture the local mine stiffness and the strain energy stored around damage zones, which are critical factors for rockbursts. Also, the estimated ppv should only be applicable to far-field areas.

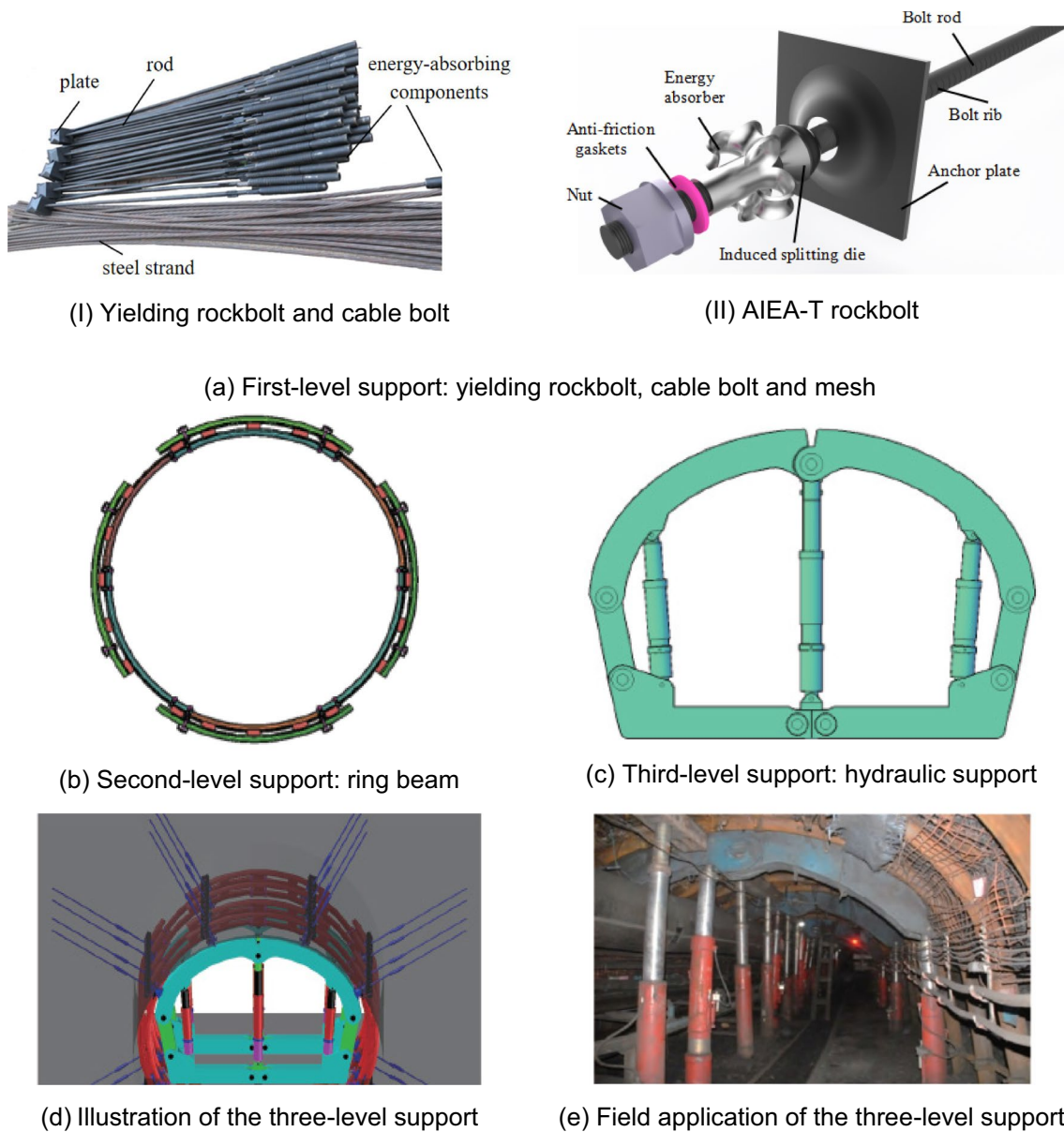


Fig. 13 Three-level energy absorption support used in severe coal burst roadway (Dai et al. 2020; Pan et al. 2020b; Qi et al. 2020)

4.4 Three-level support approach in burst-prone coal mines in China

Recently, three-level energy absorption support has been widely applied in roadways in burst-prone coal mines in China (Wei et al. 2018; Pan et al. 2020b; Qi et al. 2020; Kang. 2021), as shown in Fig. 13.

The first-level support consists of yielding reinforcements (rockbolts and cable bolts) and mesh. Fully encapsulated yielding rockbolts are applied. For example, the high strength BHRB rebar and 20MnSi rebar (discussed in Sect. 3.2) are widely used in coal excavations with high stress conditions (Kang et al. 2020). For burst-prone areas

subjected to seismic events with 100 to 1000 kJ of seismic energy, the second-level support (ring beam) is added (Pan et al. 2020b). The ring beam aims to generate yielding deformation in the circumferential direction, with maximum capacity of 1.2 m of displacement and 120 kJ to 200 kJ of energy absorption. For seismic events with seismic energy exceeding 1000 kJ, the third-level support (i.e., hydraulic support) is needed, which can provide yieldable support load in the vertical axial direction along the roadway. The hydraulic support can provide a total load resistance of 6000 kN, 200 mm of yield deformation and 1000 kJ of energy absorption (Pan et al. 2013, 2014, 2020b).

For extreme roadway conditions, the first-level support needs to be strengthened by adding mesh straps, large plates, and high pretension (above 50% of yielding load) for both rockbolts and cable bolts. The roadways need to be reinforced completely for the full cross-section, including roof, ribs and floor, as severe floor heave often occurs during coal bursts (Kang et al. 2015). Furthermore, distress blasting and distress drilling with large boreholes ranging from diameter of 120 mm to 300 mm are applied together with the three-level support in ribs and floor to reduce the high stress concentration and strain energy stored around the excavations (Kang et al. 2015; Pan et al. 2020a). Although the three-level support performs well in burst-prone coal mines, limited studies (e.g., analytical or empirical rating scheme) have been conducted for quantitatively selecting the support elements and support levels. Users need to determine the support systems based on their own experience and understanding of the specific geological and geotechnical conditions.

It is still challenging to develop a successful ground support strategy for rockburst mines, as all support design approaches have certain limitations. For the analytical approach, it is difficult to quantitatively determine both the support demand and ground support capacities in dynamic ground conditions. Empirical approaches are thus an alternative tool for designing support systems in rockburst mines. They assess the performance of the support system in areas subjected to seismic loading, and then upgrade the existing support system accordingly. However, the empirical approach needs a large amount of qualified data, and the obtained empirical parameters are often site-specific (Stacey 2012; Potvin and Hadjigeorgiou 2020). Furthermore, most empirical parameters and approaches are based on the ground support performance in burst-prone hard rock mines. Minimal empirical support design has been conducted in burst-prone coal mine conditions. Thus, in future study, a more systematic and comprehensive rating system is needed, which can provide quantitative assessment of support performance of various ground support elements in coal burst conditions. In addition, gas pressure, as one of the main components in coal (e.g., outburst), needs to be considered in the rating system.

5 Conclusions

This paper investigated ground support requirements in coal burst-prone mines. Ground support principles and considerations in burst-prone areas were first identified. The support capacities of various yielding support elements, including rockbolts, mesh, mesh straps and integrated support systems, were assessed. International best-practice ground support systems in burst-prone mines for both coal and hard rock were discussed.

In burst-prone ground conditions, the ground support system aims to maximize the capacity of accommodating rock fracturing and, in turn, to decrease the magnitude of kinetic energy of the ejected material. Three main principles are well-acknowledged in burst-prone areas: use yielding support elements, address the weakest link, and establish an integrated support system. It is crucial to ensure the deformation compatibility between each support element within a support system. As such, the support system can reach the highest possible dynamic support capacity, instead of failing at the weakest link while the yielding rockbolts have not even reached their yielding state.

With the development of yielding reinforcements in recent decades, many yielding rockbolts can provide more than 300 mm of yielding displacement and load capacity greater than 100 kN, which was a critical requirement proposed by Kaiser et al. (1996) for yielding bolts in burst-prone areas. Apart from the energy absorption and yielding deformation capacity, the initial stiffness and energy absorption rate are also critical factors when applying yielding rockbolts in practice. Stretching yielding rockbolts perform well for both the initial stiffness and energy absorption rate. For ground support systems, the combination of chain-link mesh and yielding rockbolts were classified as high support capacity (greater than 15 kJ/m² of energy absorption and 100 mm of mesh deflection). Furthermore, adding rope lacing and mesh strap to surface support elements can substantially enhance the support performance of the support system.

In practice, the Canadian Rockburst Handbook (CRH) and WASM adopt semi-analytical approaches to assess support demand in burst-prone areas and then to select support elements based on the laboratory test results. Alternatively, the empirical approaches, such as the rock damage potential method, determine the ground support elements according to the empirical rating scheme established for ground support elements and systems. In addition, a three-level support approach performs well in burst-prone coal mines in China. The levels of ground support system are generally upgraded with increasing magnitude of seismic events. Nevertheless, a more systematic and comprehensive rating scheme is needed to provide quantitative assessment of support performance of various ground support elements in coal burst conditions.

Open Access This article is licensed under a Creative Commons Attribution 4.0 International License, which permits use, sharing, adaptation, distribution and reproduction in any medium or format, as long as you give appropriate credit to the original author(s) and the source, provide a link to the Creative Commons licence, and indicate if changes were made. The images or other third party material in this article are included in the article's Creative Commons licence, unless indicated otherwise in a credit line to the material. If material is not included in the article's Creative Commons licence and your intended use is not permitted by statutory regulation or exceeds the permitted use, you will

need to obtain permission directly from the copyright holder. To view a copy of this licence, visit <http://creativecommons.org/licenses/by/4.0/>.

References

- Brändle R, Rorem E, Luis R, Fischer, G (2017) Full-scale dynamic tests of a ground support system using high-tensile strength chain-link mesh in El Teniente mine, Chile. In: Proceedings first international conference on underground mining technology, pp 25–43 (Australian Centre for Geomechanics)
- Bucher R, Cala M, Zimmermann A, Balg C, Roth A (2013) Large scale field tests of high-tensile steel wire mesh in combination with dynamic rockbolts subjected to rockburst loading. In: Proceedings seventh international symposium on ground support in mining and underground construction, pp 221–232 (Australian Centre for Geomechanics)
- Cai M (2013) Principles of rock support in burst-prone ground. *Tunn Undergr Sp Tech* 36:46–56
- Cai M, Kaiser P (2018) Rockburst support reference book—volume I: rockburst phenomenon and support characteristics, (Laurentian University: Sudbury, Canada)
- Cai W, Dou L, Si G, Hu Y (2021) Fault-induced coal burst mechanism under mining-induced static and dynamic stresses. *Engineering* 7(5):687–700
- Castro L, Bewick R, Carter T (2012) An overview of numerical modelling applied to deep mining. *Innov Numer Model Geomech* 2012:393–414
- Charette F, Plouffe M (2007) Roofex®—Results of laboratory testing of a new concept of yieldable tendon, in *Proceedings Fourth International Seminar on Deep and High Stress Mining*, Perth, Australia, pp 395–404 (Australian Centre for Geomechanics)
- Chen J, Li D (2021) Numerical simulation of fully encapsulated rock bolts with a tri-linear constitutive relation. *Tunn Undergr Sp Tech*, 104265
- Chen J, Liu P, Zhao H, Zhang C, Zhang J (2021) Analytical studying the axial performance of fully encapsulated rock bolts. *Eng Fail Anal* 128: 105580
- Dai L, Pan Y, Li Z, Wang A, Xiao Y, Liu F, Shi T, Zheng W (2021) Quantitative mechanism of roadway rockbursts in deep extra-thick coal seams: theory and case histories. *Tunn Undergr Sp Technol* 111: 103861
- Dai L, Pan Y, Wang A, Xiao Y, Ma X (2020) Experimental study on the self-protection performance of anchor bolts with energy-absorbing tails. *Rock Mech Rock Eng* 53(5):2249–2263
- Deng J, Gu D (2018) Buckling mechanism of pillar rockbursts in underground hard rock mining. *Geomech Geoeng* 13(3):168–183
- Dou L, Mu Z, Cao A, Gong S, He H, Lu C (2017) Rockburst prevention and control of coal mine. Beijing, Science Press
- Drover C, Villaescusa E (2015) Performance of shotcrete surface support following dynamic loading of mining excavations. In: Proceedings shotcrete for underground support XII, Singapore
- Drover C, Villaescusa E (2016) Estimation of dynamic load demand on a ground support scheme due to a large structurally controlled violent failure: a case study. *Min Technol* 125(4):191–204
- Duan W, Wesseloo J, Potvin Y (2015a) Evaluation of the adjusted rockburst damage potential method for dynamic ground support selection in extreme rockburst conditions. In: Proceedings international seminar on design methods in underground mining, pp 399–418 (Australian Centre for Geomechanics)
- Duan W, Wesseloo J, Potvin Y (2015b) Evaluation of the adjusted rockburst damage potential method for dynamic ground support selection in extreme rockburst conditions. In: Proceedings of the international seminar on design methods in underground mining, pp 399–418 (Australian Centre for Geomechanics)
- Galvin JM (2016) Ground engineering principles and practices for underground coal mining, (Springer)
- Gao F, Kaiser PK, Stead D, Eberhardt E, Elmo D (2019) Strainburst phenomena and numerical simulation of self-initiated brittle rock failure. *Int J Rock Mech Min Sci* 116:52–63
- Güler G, Kuijpers J, Wojno L, Milev A, Haile A (2001) Determine the effect of repeated dynamic loading on the performance of tunnel support systems. Safety in Mines Research Advisory Committee
- Hadjigeorgiou J, Potvin Y (2007) Overview of dynamic testing of ground support. In: Proceedings of the fourth international seminar on deep and high stress mining, Perth, pp 349–371 (Australian Centre for Geomechanics)
- Hadjigeorgiou J, Potvin Y (2011) A critical assessment of dynamic rock reinforcement and support testing facilities. *Rock Mech Rock Eng* 44(5):565–578
- Hao Y, Wu Y, Ranjith P, Zhang K, Hao G, Teng Y (2020) A novel energy-absorbing rock bolt with high constant working resistance and long elongation: principle and static pull-out test. *Constr Build Mater* 243: 118231
- He H, Dou L, Fan J, Du T, Sun X (2012a) Deep-hole directional fracturing of thick hard roof for rockburst prevention. *Tunn Undergr Sp Tech* 32:34–43
- He M, Gong W, Wang J, Qi P, Tao Z, Du S, Peng Y (2014) Development of a novel energy-absorbing bolt with extraordinarily large elongation and constant resistance. *Int J Rock Mech Min Sci* 67:29–42
- He M, Xia H, Jia X, Gong W, Zhao F, Liang K (2012b) Studies on classification, criteria and control of rockbursts. *J Rock Mech Geotech Eng* 4(2):97–114
- Heal D (2010) Observations and analysis of incidences of rockburst damage in underground mines, Ph.D. Thesis, University of Western Australia
- Heal D, Hudyma M, Potvin Y (2006) Evaluating rockburst damage potential in underground mining. In: Proceedings golden rocks 2006, 41st US symposium on rock mechanics (USRMS) (American Rock Mechanics Association)
- Hebblewhite B, Galvin J (2017) A review of the geomechanics aspects of a double fatality coal burst at Austar Colliery in NSW, Australia in April 2014. *Int J Min Sci Technol* 27(1):3–7
- Hedley DGF (1992) Rockburst handbook for Ontario hardrock mines. (Canmet)
- Hudyma M, Potvin YH (2010) An engineering approach to seismic risk management in hardrock mines. *Rock Mech Rock Eng* 43(6):891–906
- Iannacchione A, Tadolini SC (2016) Occurrence, prediction, and control of coal burst events in the US. *Int J Min Sci Technol* 26(1):39–46
- Iannacchione A, Zelanko J (1995) Occurrence and remediation of coal mine bumps: a historical review. In: Proceedings mechanics and mitigation of violent failure in coal and hard-rock mines, pp 27–67 (U.S. Bureau of Mines)
- Jager A, Wojno L, Henderson N (1990) New developments in the design and support of tunnels under high stress. In: Proceedings technical challenges in deep-level mining, South Africa, pp 1155–1172
- Jiang Y, Pan Y, Jiang F, Dou L, Ju Y (2014) State of the art review on mechanism and prevention of coal bumps in China. *J China Coal Soc* 39(2):205–213
- Jiang Y, Zhao Y, Wang H, Zhu J (2017) A review of mechanism and prevention technologies of coal bumps in China. *J Rock Mech Geotech Eng* 9(1):180–194

- Kaiser P, Cai M (2013) Critical review of design principles for rock support in burst-prone ground—time to rethink! In: Proceedings seventh international symposium on ground support in mining and underground construction, pp 3–37 (Australian Centre for Geomechanics)
- Kaiser P, Tannant D, McCreath D, Jesenak P (1992) Rockburst damage assessment procedure. In: Proceedings international symposium on rock support, pp 639–647
- Kaiser PK (1996) Canadian rockburst support handbook: 1996, (Geomechanics Research Centre)
- Kaiser PK (2006) Rock mechanics considerations for construction of deep tunnels in brittle rock. In: Proceedings 4th Asian rock mechanics symposium, Singapore, pp 47–58 (World Scientific)
- Kaiser PK, Cai M (2012) Design of rock support system under rockburst condition. *J Rock Mech Geotech Eng* 4(3):215–227
- Kaiser PK, MacCreath DR, Tannant DD (1996) Canadian rockburst support handbook, (Geomechanics Research Centre: Laurentian University, Sudbury, Ontario)
- Kang H (2021) Seventy years development and prospects of strata control technology for coal mine roadways in China. *Chin J Rock Mech Eng* 40(1):1–30
- Kang H, Jiang P, Huang B, Guan X, Wang Z, Wu Y, Gao F, Yang J, Cheng L, Zheng Y (2020) Roadway strata control technology by means of bolting-modification destressing in synergy in 1 000 M deep coal mines. *J China Coal Soc* 45(03):845–864
- Kang H, Wu Y, He J, Fu Y (2015) Rock bolting performance and field practice in deep roadway with rock burst. *J China Coal Soc* 40(10):2225–2233
- Konicek P, Konecny P, Ptacek J (2011) Destress rock blasting as a rockburst control technique. In: Proceedings 12th ISRM congress (international society for rock mechanics)
- Kuijpers J, Milev A, Jager A, Acheampong E (2002) Performance of various types of containment support under quasi-static and dynamic loading conditions, Part I
- Kusui A, Villaescusa E, Funatsu T (2016) Mechanical behaviour of scaled-down unsupported tunnel walls in hard rock under high stress. *Tunn Undergr Sp Tech* 60:30–40
- Li CC (2012) Performance of D-bolts under static loading. *Rock Mech Rock Eng* 45(2):183–192
- Li CC (2017a) Principles of rockbolting design. *J Rock Mech Geotech Eng* 9(3):396–414
- Li CC (2017b) Rockbolting: principles and applications. (Butterworth-Heinemann)
- Li CC (2021) Principles and methods of rock support for rockburst control. *J Rock Mech Geotech Eng* 13(1):46–59
- Li CC, Doucet C (2012) Performance of D-bolts under dynamic loading. *Rock Mech Rock Eng* 45(2):193–204
- Li CC, Hadjigeorgiou J, Mikula P, Knox G, Darlington B, Royer R, Pytlik A, Hosp M (2021) Performance of identical rockbolts tested on four dynamic testing rigs employing the direct impact method. *J Rock Mech Geotech Eng*
- Li CC, Mikula P, Simser B, Hebblewhite B, Joughin W, Feng X, Xu N (2019) Discussions on rockburst and dynamic ground support in deep mines. *J Rock Mech Geotech Eng* 11(5):1110–1118
- Li CC, Stjern G, Myrvang A (2014) A review on the performance of conventional and energy-absorbing rockbolts. *J Rock Mech Geotech Eng* 6(4):315–327
- Li L, Li F, Zhang Y, Yang D, Liu X (2020) Formation mechanism and height calculation of the caved zone and water-conducting fracture zone in solid backfill mining. *Int J Coal Sci Technol* 7(1):208–215
- Mark C (2016) Coal bursts in the deep longwall mines of the United States. *Int J Coal Sci Technol* 3(1):1–9
- Martínez L, Sepúlveda N, Marulanda Y, Valdivieso J, Contreras J (2020) Critical review on the dynamic energy dissipation capacity of surface support elements. In: Proceedings MassMin2020, Santiago, Chile
- Masoudi R, Sharifzadeh M (2018) Reinforcement selection for deep and high-stress tunnels at preliminary design stages using ground demand and support capacity approach. *Int J Min Sci Technol* 28(4):573–582
- Mazaira A, Konicek P (2015) Intense rockburst impacts in deep underground construction and their prevention. *Can Geotech J* 52(10):1426–1439
- Mercier-Langevin F, Hadjigeorgiou J (2011) Towards a better understanding of squeezing potential in hard rock mines. *Min Technol* 120(1):36–44
- Mikula P (2012) Progress with empirical performance charting for confident selection of ground support in seismic conditions. *Min Technol* 121(4):192–203
- Milev S (2005) Strong ground motion and site response in deep South African mines. *J South Afr Inst Min Metall* 105(7):515–524
- Morissette P, Hadjigeorgiou J (2019) Ground support design for dynamic loading conditions: a quantitative data-driven approach based on rockburst case studies. *J Rock Mech Geotech Eng* 11(5):909–919
- NCM (2019) PAR1 bolt brochure. New Concept Mining. https://www.ncm.co.za/downloads/brochure/6734_NCM_PAR1_Bolt_Brochure_SA_BR017-R05.pdf
- NGI (2015) Using Q-system-rock mass classification and support design. Norwegian Geotechnical Institute
- Ortlepp W (1968) A yielding rockbolt, Research Organisation Bulletin of the Chamber of Mines of South Africa, 14, 6–8
- Ortlepp W (1992) The design of support for the containment of rockburst damage in tunnels—an engineering approach. In: Kaiser PK, McCreath DR (eds) Rock support in mining and underground construction. Balkema, Rotterdam
- Ortlepp W (1993) High ground displacement velocities associated with rockburst damage. In: Proceedings rockbursts and seismicity in mines 93: proceedings of the 3rd international symposium, Kingston, Ontario, pp 101–106
- Ortlepp W (2005) RaSiM comes of age: a review of the contribution to the understanding and control of mine rockbursts. In: Proceedings of the sixth international symposium on rockburst and seismicity in mines, Perth, Western Australia, pp 9–11
- Ortlepp W (2006) Comment on the paper ‘Strong ground motion and site response in Deep South African Mines’, by SM Spottiswood and AM Milev. *J South Afr Inst Min Metall* 106:593–597
- Ortlepp W, Stacey T (1994) Rockburst mechanisms in tunnels and shafts. *Tunn Undergr Sp Tech* 9(1):59–65
- Ortlepp W, Stacey T (1998) Performance of tunnel support under large deformation static and dynamic loading. *Tunn Undergr Sp Tech* 13(1):15–21
- Ortlepp WD (1997) Rock fracture and rockbursts: an illustrative study, (South African Institute of Mining and Metallurgy: Johannesburg)
- Pan J, Qi Q, Liu S, Wang S, Ma W, Kang X (2020a) Characteristics, types and prevention and control technology of rock burst in deep coal mining in China. *J China Coal Soc* 45(1):111–121
- Pan Y, Qi Q, Wang A, Xiao Y, Chen J, Lv X, Xu L, Dai L (2020b) Theory and technology of three levels support in bump-prone roadway. *J China Coal Soc* 45(5):1585–1594
- Pan Y, Wang K, Xiao Y (2013) Design of anti-scour support based on theory of pendulum-type wave. *Chin J Rock Mech Eng* 8:005
- Pan Y, Xiao Y, Li Z, Wang K (2014) Study of tunnel support theory of rockburst in coal mine and its application. *J China Coal Soc* 39(2):222–228
- Player J, Thompson A, Villaescusa E (2008) Dynamic testing of reinforcement systems. In: Proceedings 6th international

- symposium on ground support in mining and civil engineering construction, pp 597–622
- Player J, Villaescusa E, Thompson A (2004) Dynamic testing of rock reinforcement using the momentum transfer concept. In: Proceedings 5th international symposium of rock support and reinforcement, Australia
- Potvin Y (2009) Strategies and tactics to control seismic risks in mines. *J South Afr Inst Min Metall* 109(3):177–186
- Potvin Y, Hadjigeorgiou, J (2020) Ground support for underground mines, (Australian Centre for Geomechanics: Perth)
- Potvin Y, Wesseloo J (2013) Towards an understanding of dynamic demand on ground support. *J South Afr Inst Min Metall* 113(12):913–922
- Potvin Y, Wesseloo J, Heal D (2010) An interpretation of ground support capacity submitted to dynamic loading. *Min Technol* 119(4):233–245
- Qi Q, Pan Y, Li H, Jiang D, Shu L, Zhao S, Zhang Y, Pan J, Li H, Pan P (2020) Theoretical basis and key technology of prevention and control of coal-rock dynamic disasters in deep coal mining. *J China Coal Soc* 45(5):1567–1584
- Salamon M, Wagner H (1979) Role of stabilizing pillars in the alleviation of rock burst hazard in deep mines. In: Proceedings 4th ISRM Congress (International Society for Rock Mechanics)
- Sharifzadeh M, Lou J, Crompton B (2020) Dynamic performance of energy-absorbing rockbolts based on laboratory test results. Part I: evolution, deformation mechanisms, dynamic performance and classification. *Tunn Undergr Sp Tech* 105(2020): 103510
- Si G, Belle B (2019) Performance analysis of vertical goaf gas drainage holes using gas indicators in Australian coal mines. *Int J Coal Geol*, 216, 103301
- Si G, Cai W, Wang S, Li X (2020) Prediction of relatively high-energy seismic events using spatial–temporal parametrisation of mining-induced seismicity. *Rock Mech Rock Eng* 53(11):5111–5132
- Simon R (2001) Analysis of fault-slip mechanisms in hard rock mining, PhD thesis, McGill University
- Simser B (2007) The weakest link-Ground support observations at some Canadian Shield hard rock mines. In: Proceedings fourth international seminar on deep and high stress mining, pp 335–348 (Australian Centre for Geomechanics)
- Smith JA, Ramandi HL, Zhang C, Timms W (2019) Analysis of the influence of groundwater and the stress regime on bolt behaviour in underground coal mines. *Int J Coal Sci Technol* 6(2):286–300
- Song Z, Frühwirth T, Konietzky H (2020) Inhomogeneous mechanical behaviour of concrete subjected to monotonic and cyclic loading. *Int J Fatigue*, 132: 105383
- Song Z, Wang Y, Konietzky H, Cai X (2021) Mechanical behavior of marble exposed to freeze-thaw-fatigue loading. *Int J Rock Mech Min Sci* 138: 104648
- Stacey T (2012) A philosophical view on the testing of rock support for rockburst conditions. *J South Afr Inst Min Metallur* 112(8):01–08
- Stacey T, Ortlepp W (2001) Tunnel surface support-capabilities of various types of wire mesh and shotcrete under dynamic loading. *J South Afr Inst Min Metallur* 101(7):337–342
- Suorinen F, Hebblewhite B, Saydam S (2014) Geomechanics challenges of contemporary deep mining: a suggested model for increasing future mining safety and productivity. *J South Afr Inst Min Metall* 114(12):1023–1032
- Tang B (2000) Rockburst control using destress blasting. Ph.D. thesis, McGill University Montreal
- Thompson A, Villaescusa E, Windsor C (2012) Ground support terminology and classification: an update. *Geotech Geol Eng* 30(3):553–580
- Turcotte P (2014) Practical applications of a rockburst database to ground support design at LaRonde Mine. In: Proceedings seventh international conference on deep and high stress mining, pp 79–91 (Australian Centre for Geomechanics)
- Turner M, Green T (2005) Threadbar bolts in a seismically active, high stress, high yield environment—Otter-Juan Mine, Kambalda. In: Proceedings sixth international symposium on rockburst and seismicity in mines, Australian Centre for Geomechanics, Perth, pp 67–73
- Turner M, Player J (2000) Seismicity at big bell mine. In: Proceedings of MassMin. Australasian Institute of Mining and Metallurgy
- Vardar O (2019) Assessment of effects of geological and geotechnical factors on coal burst proneness, Ph.D. thesis, University of New South Wales, Sydney
- Villaescusa E, Kusui A, Drover C (2016) Ground support design for sudden and violent failures in hard rock tunnels. In: Proceedings 9th Asian rock mechanics symposium, pp 18–20
- Villaescusa E, Thompson A, Player J (2013) A decade of ground support research at the WA School of Mines. In: Proceedings seventh international symposium on ground support in mining and underground construction, pp 233–245 (Australian Centre for Geomechanics)
- Villaescusa E, Thompson A, Player J, Morton E (2015) Dynamic testing of ground support systems. Minerals and Energy Research Institute of Western Australia
- Wang A, Gao Q, Dai L, Pan Y, Zhang J, Chen J (2018) Static and dynamic performance of rebar bolts and its adaptability under impact loading. *J China Coal Soc* 43(11):2999–3006
- Wang G, Wu X, Jiang Y, Huang N, Wang S (2013) Quasi-static laboratory testing of a new rock bolt for energy-absorbing applications. *Tunn Undergr Sp Tech* 38:122–128
- Wei C, Zhang C, Canbulat I (2020) Numerical analysis of fault-slip behaviour in longwall mining using linear slip weakening law. *Tunn Undergr Sp Tech*, 104: 103541
- Wei C, Zhang C, Canbulat I, Cao A, Dou L (2018) Evaluation of current coal burst control techniques and development of a coal burst management framework. *Tunn Undergr Sp Tech* 81:129–143
- Wei C, Zhang C, Canbulat I, Huang W (2021) Numerical investigation into impacts of major fault on coal burst in longwall mining: a case study. *Int J Rock Mech Min Sci* 147: 104907
- Wu Y, Oldsen J (2010) Development of a new yielding rock bolt-Yield-Lok bolt. In: Proceedings 44th US rock mechanics symposium and 5th US-Canada Rock mechanics symposium, Salt Lake City (American Rock Mechanics Association)
- Xue D, Zhou J, Liu Y, Gao L (2020) On the excavation-induced stress drop in damaged coal considering a coupled yield and failure criterion. *Int J Coal Sci Technol* 7(1):58–67
- Zhang C, Canbulat I, Hebblewhite B, Ward CR (2017) Assessing coal burst phenomena in mining and insights into directions for future research. *Int J Coal Geol* 179:28–44
- Zhang P, Swan G, Nordlund E (2015) 1D numerical simulation of velocity amplification of P-waves travelling through fractured rock near a free surface. *J South Afr Inst Min Metall* 115(11):1121–1126
- Zhang S, Lu L, Wang Z, Wang S (2020) A physical model study of surrounding rock failure near a fault under the influence of footwall coal mining. *Int J Coal Sci Technol* 8(4):626–640
- Zhou J, Li X, Mitri HS (2018) Evaluation method of rockburst: state-of-the-art literature review. *Tunn Undergr Sp Tech* 81:632–659
- Zuo J, Wang J, Jiang Y (2019) Macro/meso failure behavior of surrounding rock in deep roadway and its control technology. *Int J Coal Sci Technol* 6(3):301–319